LUBRICATION SCIENCE
Lubrication Science 2017; **29**:133–152
Published online 7 November 2016 in Wiley Online Library (wileyonlinelibrary.com). DOI: 10.1002/ls.1361

An analytical approach on the tribological behaviour of pocketed slider bearings with boundary slip including cavitation

M. Muchammad[1,2,*,†], Mohammad Tauviqirrahman[2], J. Jamari[2] and Dirk Jan Schipper[1]

[1]*Laboratory for Surface Technology and Tribology, Faculty of Engineering Technology, University of Twente, Enschede, The Netherlands*
[2]*Laboratory for Engineering Design and Tribology, Department of Mechanical Engineering, University of Diponegoro, Semarang, Indonesia*

ABSTRACT

Slider bearing performance depends on the boundary conditions at the interface between the solid surfaces and the fluid. This paper presents the combined effect of pockets and boundary slip on the load support and friction of parallel sliding systems using analytical solutions for a simple pocketed bearing. The effect of cavitation was of particular interest with respect to the inlet suction mechanism. It was demonstrated that applying boundary slip in a pocketed slider bearing gives a reduction in load support compared with the textured bearing without wall slip. Adding slip over the whole surface could retard the presence of cavitation. The influence of boundary slip is explored, and was found to significantly affect the frictional behaviour. Copyright © 2016 John Wiley & Sons, Ltd.

Received 14 April 2015; Revised 31 August 2016; Accepted 9 October 2016

KEY WORDS: analytical method; slider bearing; slip; load support; friction

NOMENCLATURE

a = inlet length
b = pocket width
B_o = slider length
c = outlet land length
F_f = friction
h_1 = film thickness at A
h_2 = inlet land film thickness at B
h_{2p} = film thickness in pocket at B
h_3 = film thickness in outlet land at C

*Correspondence to: M. Muchammad, Laboratory for Engineering Design and Tribology, Department of Mechanical Engineering, University of Diponegoro, Jl. Prof. Soedharto, SH., Tembalang, Semarang 50275, Indonesia.
†E-mail: m_mad5373@yahoo.com

h_{3p} = film thickness in pocket at C
h_d = height of microtexture pocket (excluding film thickness)
h_o = minimum film thickness in inlet land at B
P_2 = pressure at B
P_3 = pressure at C
P_{atm} = atmospheric pressure
P_{cav} = cavitation pressure
U = sliding velocity
W = load support
q = flow rate
x = coordinate in sliding direction
X_b = non-cavitated fraction of pocket breadth
z = coordinate through film thickness
μ = lubricant dynamic viscosity
α_s, α_h = slip coefficient at surface s (moving) and h (stationary)

INTRODUCTION

Surface texturing is an effective approach to increase the tribological performance of lubricated mechanical components. It is known that by introducing textured surfaces it significantly can affect friction and load support of sliding bearings. In recent years, a great deal of effort has been addressed to investigate the influence of the texture's geometric parameters. It was shown experimentally that such texturing enhances load support and reduces hydrodynamic friction for instance systems with two parallel sliding surfaces,[1,2] mechanical seals[3] and reciprocating (cylinder-liner) contacts.[4]

The effect of surface texturing on the tribological performance has been analysed numerically by many researchers such as Arghir et al.,[5] Sahlin et al.,[6] Brajdic-Mitidieri et al.,[7] Kligerman et al.,[8] Fowell et al.,[9] Dobrica and Fillon[10] and Han et al.[11] There are two approaches for the investigation of textured surfaces, i.e. using CFD models based on Navier–Stokes[5–7,10,11] and using Reynolds.[6,8–10] Sahlin et al.[6] confirmed that by using CFD the introduction of a micro-groove on the stationary surface of a parallel slider leads to a net pressure build-up and hydrodynamic load support. In their research, it was found that the effect of inertia on lubrication was dominant. Similarly, Han et al.[11] reported a three-dimensional CFD analysis of a spherical dimple on the stationary surface of a parallel sliding contact. An optimum micro dimple (depth and width) is defined which gives the largest load support and smallest coefficient of friction. Brajdic-Mitidieri et al.[7] used the Navier–Stokes equation combined with a cavitation model to analyse the lubricant behaviour in plain bearing pad bearings having a closed pocket. Such texture could produce a reduction in the friction coefficient and increase in load support. This effect depends on the bearing convergence ratio (inlet over outlet film thickness). It should be pointed out that these analyses[5–7,11] only focused on single texture cells with centered dimples. Such configurations can lead to wrong conclusions in the prediction of hydrodynamic performance concerning the inertia effect.[10]

In the case of multiple cells in hydrodynamic parallel sliding textured surfaces, Dobrica and Fillon[10] conducted a parametric study on the texturing parameters, dimension (depth and width), number and density of the cells to improve the hydrodynamic performance. They analysed the

DOI: 10.1002/ls

validity of the Reynolds equation and inertia effects in parallel textured sliders of infinite width using the Reynolds equation and commercial CFD simulation software (FLUENT). Among the original conclusions of this study that inertia was noted to have a negative effect when applied to partially textured surfaces, i.e. reduced load support which was also found for the fully textured configurations. This result contradicts with the works of Refs.[5–7,11] in the case of two parallel moving surfaces with a single cell texture, and the work of Kligerman et al.[8] in the case of the contact between a piston ring and cylinder liner with applying multiple texture cells. It was demonstrated that there is an advantage of partial texturing over full texturing of the surface in view of friction using a theoretical model based on a modified Reynolds equation.[8] A load support mechanism between parallel sliding surfaces was proposed by Fowell et al.[9] They showed that the inlet suction mechanism in textured hydrodynamic bearings that has micropockets on its surface provides enhanced load support and reduced friction.

In most theoretical studies cited above, it has been assumed that the lubricated contact was represented by no-slip planes. Obviously, this assumption simplified the theoretical analysis and was successfully applied to engineering problems to some extent. However, with the continuous progress of the nano measurement techniques during recent years, a nano scale measurement is possible with respect for the wall slip.[12–14]

Recently, in addition to surface texturing, the use of an artificial slip surface is also of great interest with respect to lubrication. Such surface was introduced and applied to bearings with the help of microfabrication techniques. On micro scale such as in Micro-Electro-Mechanical-System (MEMS), the boundary condition, i.e. slip or no-slip situation, will play a very important role in determining the fluid flow behaviour. Control of the boundary condition will allow a degree of control over the hydrodynamic pressure in confined systems and be important in a lubricated sliding contact. How to control the wall slip was one of the challenging research questions in recent investigations. However, in tribological lubricated system such as in bearing, the presence of the slip can be engineered in certain area by modifying the contacting surfaces. Based on literature survey, at least there are three mechanisms which lead to the presence of the slip. First, the slip exists due to the effect of wetting and surface energy[15–18]. Second, the slip occurs due to the surface topography, i.e. low roughness as suggested by some researchers[17,19]. Third, one can add components (additives) to a base oil to generate wall slip as investigated by Spikes and his group[20,21]. As a remark, it is clear that at macro scale, the roughness and wetting properties have a significant role to promote the slip at the wall in lubricated systems. Also, in grease lubricated systems in which the film formation is governed by the base oil viscosity, the slip phenomenon can be controlled by modifying the roughness[22,23].

Several researchers such as Salant and Fortier,[24] Wu et. al.[25] and Ma et al.[26,27] have explored the behaviour of the sliding contact using an optimised slip zone with respect to load support. The results of all these investigations show the existence of a lift force (load support) even there is no wedge effect (two parallel sliding surfaces) using such artificial slip zone. However, none of these studies have included surface texturing.

Very few researchers appear to have considered the interplay of surface texture and boundary slip effect on lubrication. Bayada and Meurisse[28] compared the slip/no-slip heterogeneity with roughness. They concluded that film rupture in diverging zones can be provoked by a certain artificial slip boundary configuration which is similar to that caused by geometrical roughness. However, in their study the combination of the effect of artificial slip and surface texture on the hydrodynamic behaviour was not conducted. Rao[29] employed artificial slip on a stationary surface having a single-groove at a

DOI: 10.1002/ls

slider and a journal bearing and calculated pressure and shear stress distributions. The modified Reynolds equation with the Navier–slip boundary condition was solved numerically with regard to the effect of wall slip and single groove texture simultaneously. In a recent publication, Aurelian et al.[30] investigated the influence of boundary slip on load support and power loss in hydrodynamic fluid bearings. A simple textured/boundary slip combination was investigated. The main conclusion of their study was that when choosing a texture/slip zone geometry it should be done carefully because an inappropriate choice can lead to a drastic deterioration of the bearing performance, especially in relation to the load support. However, the authors focused only on the slip property with zero critical shear stress. Tauviqirrahman et al.[31–34] explored the possibility of slip and texture in order to improve the performance characteristics. Their results indicate that the combined texture/slip pattern increase load carrying capacity and decrease friction.

In most of the previous works, the load support generation mechanisms were demonstrated using a simple simulation approach for a one-dimensional parallel bearing having a single cell texture without cavitation. Regarding the cavitation effect in the slip textured contact on the lubrication performance, it is noted that in recent literature, only Wang and Lu[35] have taken into account the cavitation effect for two-dimensional sleeve bearing. In the present study, an improvement in the performance of pocketed slider bearings is examined based on the wall slip phenomenon. The flow pattern in the bearing can be altered if the wall slip is located in a deterministic way in certain regions of the pocketed bearing surface. The modified form of the Reynolds equation containing the cavitation effect is derived in which the wall slip is allowed to occur in a textured bearing.

It is interesting to note, that when boundary slip is of particular interest in bearing analysis, for most previously published works, for example, the work of [24–27,29–34], the cavitation was neglected, and most of them used a non-mass conserving equations. As can be seen in the numerical results below, the cavitation has a significant effect and the exclusion of cavitation in mathematical model may lead to wrong conclusion. Therefore, to complement the previous findings, an analytical lubrication model with boundary slip taking into account the cavitation effect is proposed. As a note, in this paper the mechanisms of slip based on physical point of view are not investigated.

MATHEMATICAL MODEL AND ITS SOLUTION

The textured bearing configuration is shown in Figure 1. The textured surface is composed of a single recess with boundary slip. In hydrodynamic lubrication, the governing equations are described by the well-known Reynolds equation which is a simplification of Navier–Stokes equation. In Reynolds approach, the assumptions used are as follows:

1. Small film thickness relative to the contact length.
2. Non-varying pressure across the film thickness.
3. The compressibility of the fluid is negligible.
4. The flow is laminar.
5. The gravity and inertia forces acting on the fluid can be ignored compared to the viscous force.

In the present work, an analytical equation based on first-order Reynolds theory is derived. In this way, the Reynolds equation is extended by considering slip and cavitation. Here, slip is engineered to occur on the whole stationary surface thus also the pocket surface (i.e. ‘full slip’ configuration) as

DOI: 10.1002/ls

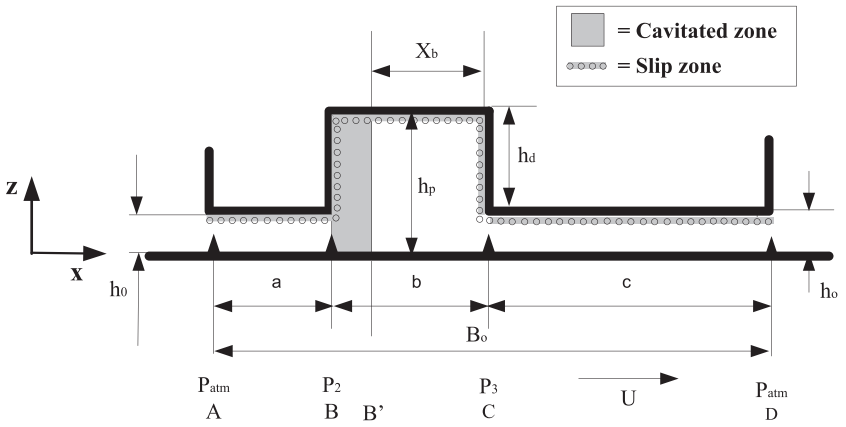

Figure 1. Schematic diagram of parallel textured bearing.

shown in Figure 1. The methodology used in the derivation of the extended Reynolds equation at the bearing surface is quite similar to that employed by Fowell[9] and is given in detail in Appendix A.

For a pocketed bearing with slip as illustrated in Figure 1, expressions of the pressure and flow rate can be obtained. Applying pressure continuity at boundary points, a set of governing equations can be obtained for the flow rate, and constants of integration in the pressure expressions, see Appendix A for details. In Appendix A, the derivation of the flow rate and pressure, which are the basis of this analysis, is presented in equations A.1–A.14. Solving the set of governing equations and employing the quantities in the nomenclature, the analytical solution for the slip case is:

$$P_2\left[\left(h_p^3+3h_p^3K_p\right)\frac{ab+bc}{ab^2}+\left(\frac{h_o^3+3h_o^3K_o}{a}\right)\right]=P_{atm}\left[\left(h_p^3+3h_p^3K_p\right)\frac{ab+bc}{ab^2}+\left(\frac{h_o^3+3h_o^3K_o}{a}\right)\right]$$
$$-6\mu U\left[\left(h_p+h_pK_p\right)-\left(h_o+h_oK_o\right)\right]. \tag{1}$$

For the analysis of a pocketed bearing with slip condition, the boundary slip is employed to all sides of the pocket cell (see Figure 1). The load support W and friction F_f are of particular interest. The derivation of load support and friction either with cavitation or no cavitation condition is given in Appendix A, i.e. equations A.15–A.22. For all the following simulations, the standard one-dimensional bearing geometry is investigated, with values for the parameter as presented in Table I.

In the present study, solving the lubrication problem for a pocketed slider bearing from numerical point of view, the solution method is proposed as follows:

1. For all computations, the cavitation phenomenon is assumed to occur in bearing. Here, the cavitation equations (equations A.21 and A.22 in Appendix A) to obtain X_b (non-cavitated region as seen in Figure 1) are used. Then, the X_b will be used an indicator whether cavitation occurs or not. It should be noted that the cavitation occurs if $0<X_b<b$ where b is pocket length.
2. If the cavitation is present in pocketed bearing, then other cavitation equations (section A.1. in Appendix A) are implemented to predict the pressure as well as the friction force.

DOI: 10.1002/ls

Table I. Characteristics of main bearing analysed

Parameters	Symbols	Value
Bearing length	B_o	0.02 m
Inlet length	a	0.004 m
Pocket length	b	0.006 m
Exit land length	c	0.01 m
Atmospheric pressure	p_{atm}	100 kPa
Cavitation pressure	p_{cav}	0–100 kPa
Sliding velocity	u	1 m/s
Slip coefficient	α	0.02 m^2s/kg

3. For the condition where the cavitation does not exist (in this case, $X_b \leq 0$ or $X_b \geq b$), then the non-cavitation equations (section A.1. in Appendix A) are used to calculate the pressure as well as the friction force.

RESULTS AND DISCUSSIONS

As discussed by Fowell et al.,[9] the existence of inlet suction with respect to the hydrodynamic lubrication mechanism has a significant effect in a textured bearing. In this paper, combining texture and wall slip on one surface will be explored in more detail.

The analysis of inlet suction is performed in full by deriving the equation for the net load support and the friction as shown in Appendix A. The main basic of derivation of this equation is by equating the flows through the three parts of the bearing. In the analysis, the pressure at the inlet of the recess must be evaluated whether it falls to the cavitation pressure or not.

Figure 2 shows the bearing load support plotted against the slip coefficient for various depth values of the pocket. It can be observed that the predicted load support is higher for a bearing having higher

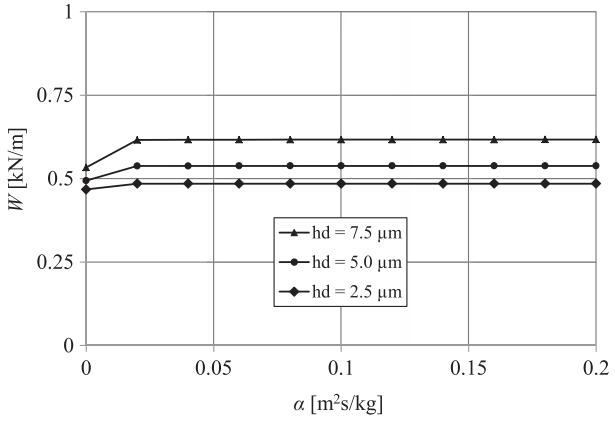

Figure 2. Influence of slip coefficient on load support for several values of pocket depth h_d (Note: $h_o = 1.0 \times 10^{-6}$ m, $a = 0.004$ m, $b = 0.006$ m, $B_o = 0.02$ m).

DOI: 10.1002/ls

h_d. This prevails either for a pocketed bearing with slip or that without slip. It matches well with previous research, for example by Fowell et al.[9] to the case of a no-slip ($\alpha = 0$) pocketed bearing. At first sight, it seems that the load support of the pocketed bearing with slip is slightly higher than that without slip ($\alpha = 0$); it is just 3–15% depending on the value of h_d. However, for all values of the pocket depth considered here, the increase in the slip coefficient does not influence the predicted load support. This is to say that the performance of the pocketed bearing with respect to the load support hardly improves by adding slip.

Figure 3 shows the influence of the minimum film thickness h_o on the load support. One area of interest is the comparison of the performance between the pocketed bearing with slip and without slip. In this figure, for each case, there is a peak that separates two areas, the cavitation area and the no-cavitation area. Open markers represent cavitated results, while for solid markers, no cavitation is present. As can be seen in this figure that in comparison with the traditional pocketed bearing, introducing slip into the pocketed slider bearing increases the load support. However, this prevails for the cavitation region. From the physical point of view, this new finding is interesting. As can be observed in Figure 4 (for example, in the case of pocketed bearing with $h_d / h_o = 0.71$), adding the boundary slip will generate a positive effect, i.e. more hydrodynamic pressure than that without boundary slip. The explanation of this effect could be that by introducing boundary slip over the whole surface could retard the level of cavitation. On the other hand, slip makes the inlet suction mechanism occur. For the non-cavitation region ($h_d / h_o = 0.31$ in this case), contradictive result is found; slip generates less pressure and thus produces the reduced load support as can be seen in more detail in Figure 5. This is as expected because the full slip configuration as investigated by other researchers[25–27,31,32] has a negative effect with respect to the load support in the absence of the cavitation. In general, based on these figures, a specific observation can be drawn, that is, the fact that the slip is able to increase the load support when cavitation occurs.

Figure 6 shows the variation of the load support with pocket depth for two conditions, i.e. slip and no-slip. As can be seen from this figure, the lubrication performance of a textured slider bearing with slip is higher than that without slip for all pocket depths. In addition, Figure 6 shows that increasing the

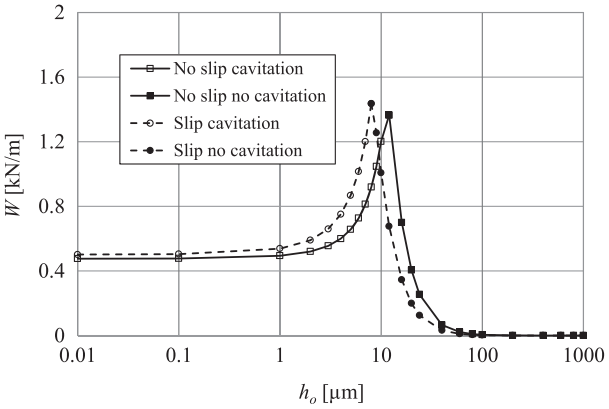

Figure 3. The load support as a function of minimum film thickness for the case of $h_d = 5.0 \times 10^{-6}$ m, $a = 0.004$ m, $b = 0.006$ m, $B_o = 0.02$ m. The slip coefficient $\alpha = 0.02$ m^{2}s/kg.

DOI: 10.1002/ls

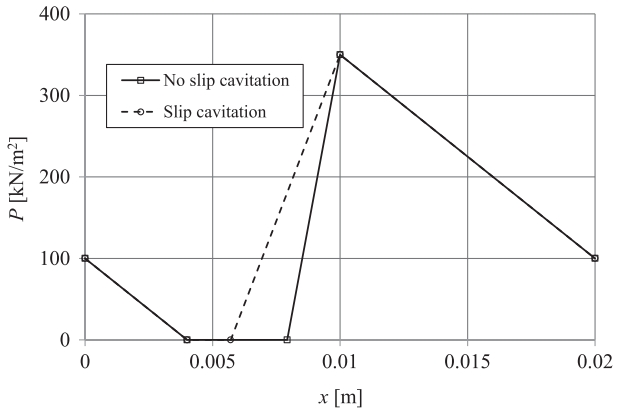

Figure 4. The pressure distribution as a function of coordinate in sliding direction for the pocketed bearing of interest with $h_d = 5.0 \times 10^{-6}$ m, $h_o = 7.0 \times 10^{-6}$ m, $a = 0.004$ m, $b = 0.006$ m, $B_o = 0.02$ m, and $\alpha = 0.02$ m^{2}s/kg. Cavitation is present.

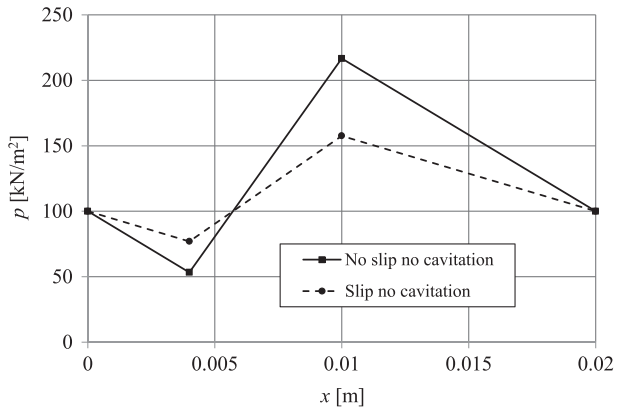

Figure 5. The pressure distribution as a function of coordinate in sliding direction for the pocketed bearing of interest with $h_d = 5.0 \times 10^{-6}$ m, $h_o = 1.6 \times 10^{-5}$ m, $a = 0.004$ m, $b = 0.006$ m, $B_o = 0.02$ m, and $\alpha = 0.02$ m^{2}s/kg. Cavitation is absent.

pocket depth results in the decrease-then-increase behaviour of the load support. This trend seems to be very clear for both conditions (slip and no-slip). For $h_d = 0.5 \times 10^{-6}$ m, a minimum in load support is achieved for both cases, 0.4638 kN/m and 0.4568 kN/m, respectively, for the slip and no-slip situation.

For low h_d (less than 2×10^{-6} m in this case), the predicted load support for both cases is very close. It can be observed that the deviation between the case of slip pocketed bearing and the no-slip pocketed bearing is lower than 8%, even when the predicted load support is calculated for the lowest h_d, i.e. 0.03×10^{-6} m, which means that the bearing pattern is very close to that of a flat bearing. In other words, by adding slip to the texture from low h_d does not influence the load support very much. From a physical point of view, it means that slip is not able to encourage the occurrence of cavitation; it is just the texture which influences the performance.

DOI: 10.1002/ls

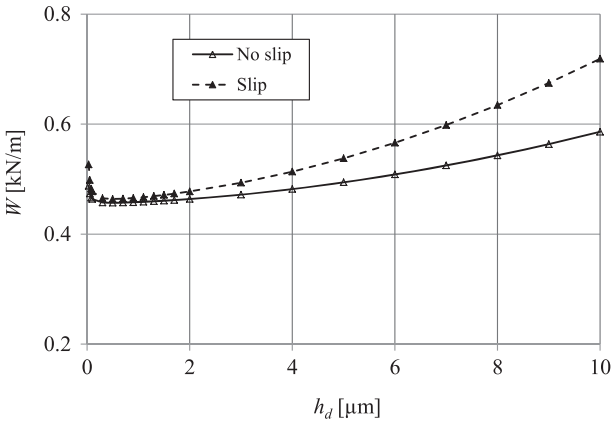

Figure 6. The load support as a function of pocket depth for the case of $h_o = 1.0 \times 10^{-6}$ m, $a = 0.004$ m, $b = 0.006$ m, $B_o = 0.02$ m. The slip coefficient $\alpha = 0.02$ m^{2}s/kg.

Figure 7 illustrates the load support which is plotted against the ratio b/B_o. As expected, for low h_d ($h_d = 2.5 \times 10^{-6}$ m in this case), the load support prediction between slip and no-slip textured bearing is very close. This is consistent with the previous results (see Figure 6). As b/B_o increases, the load support decreases. For high h_d, the difference in load support between the slip and no-slip situation is not as small as the case for low h_d, especially for b/B_o which is lower than, say, 0.1. Figure 7 also reflects that the load support for a slip textured bearing, for all h_d values considered here, is higher than that of no-slip textured bearing. With respect to the utilisation of slip (i.e. $\alpha = 0.02$ m^{2}s/kg) on a textured bearing, the load support can be improved from 1.2 to 11.8% (at $h_d = 2.5 \times 10^{-6}$ m) and 5.4 to 38.4% (at $h_d = 7.5 \times 10^{-6}$ m) depend on b/B_o. It means that the slip effect has a significant contribution on the pressure distribution and thus the load support especially when the pocket depth is high. In relation to the texture parameter (i.e. pocket depth), as is shown in Figure 7, for h_d considered here, it can be observed that the higher the pocket depth, the higher

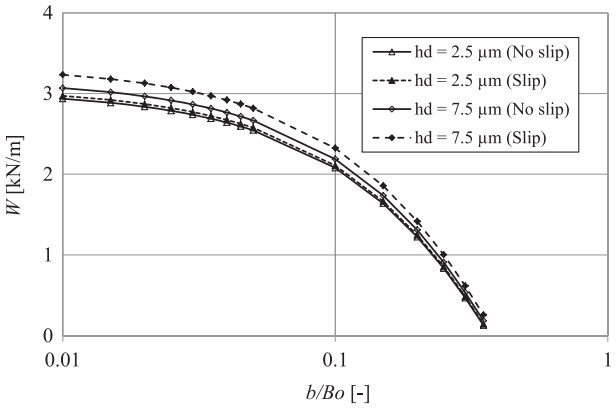

Figure 7. The effect of pocket length b/B_o on the load support W. The profiles are calculated for $h_o = 1.0 \times 10^{-6}$ m, $a = 0.004$ m, $B_o = 0.02$ m and $\alpha = 0.02$ m^{2}s/kg.

DOI: 10.1002/ls

the predicted load support, which matches well with the previous results, see Figure 6. This prevails both for the slip and no-slip textured bearing.

In Figure 8, the load support of the textured bearing (with and without slip) versus the variation of the inlet length a/B_o is presented. The results are evaluated for several pocket depths. In this figure, data points where cavitation does not take place are presented by solid markers and those where cavitation occurs are shown in open markers. It is interesting to observe that the no cavitation region for the case of slip textured bearing both for h_d of 2.5×10^{-6} m and 7.5×10^{-6} m is wider than the results for the no-slip textured bearing. It seems counterintuitive that no-slip pockets cavitate more easily at low values of a/B_o than pockets with slip. The explanation is that the lubricant can move more easily at the slip surface and fill the pocket more quickly. Thus, adding slip can reduce the presence of cavitation, and therefore it leads to improved performance of a textured bearing.

Figure 8 also shows that in relation to the effect of the pocket depth, both for the slip and no-slip surface, the deeper the pocket, the more difficult cavitation takes place. As explained by Fowell et al.,[9] for a traditional (no-slip) textured bearing, this is due to the restriction of the flow which is higher for deeper pockets than for shallow ones. It seems that this condition also prevails for the slip pocket.

Figure 9 reflects the correlation between the inlet land width a/B_o and pocket depth h_d. It can be observed that the pocket depth has a strong influence on the inlet length as the initiator for cavitation both for the slip and no-slip cases. The minimum values as the critical points of pocket depth h_d for both cases are noted. This is to say that below these pocket depth values, the lubricant in the inlet starts to reduce the amount of flow in the pocket. It is worth noting that the critical value of h_d for the slip case is higher than the no-slip case (see insert for details). Obviously, as can also be seen from Figure 9, the predicted values for a/B_o for the slip case are higher than the no-slip case for all values of h_d considered here. From a physical point of view, it indicates that adding slip to the pocket bearing enables to reduce the presence of cavitation. For example, for the no-slip textured bearing of interest with $h_d=4.0\times10^{-6}$ m and the inlet length a/B_o 0.01, lubrication will generate the cavitation phenomena. However, if the slip is applied on such bearing, the cavitation can be prevented.

Figure 10 shows the effect of the cavitation pressure on the load support. It can be observed that the trend of the load support prediction both for the case of slip and no slip is identical, that is, the decrease

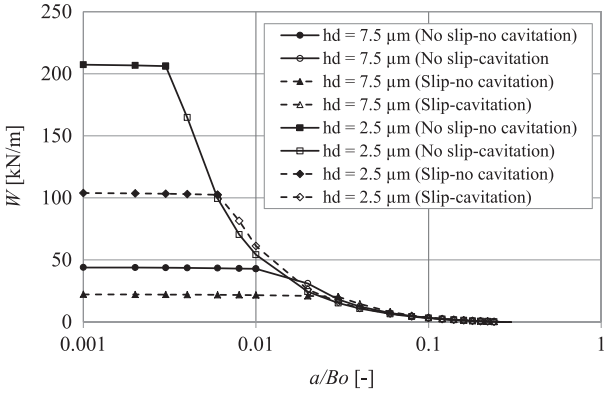

Figure 8. The effect of inlet length on the load support. The profiles are calculated for $h_o=1.0\times10^{-6}$ m, $b=0.006$ m, $B_o=0.02$ m, $\alpha=0.02$ m^{2}s/kg.

DOI: 10.1002/ls

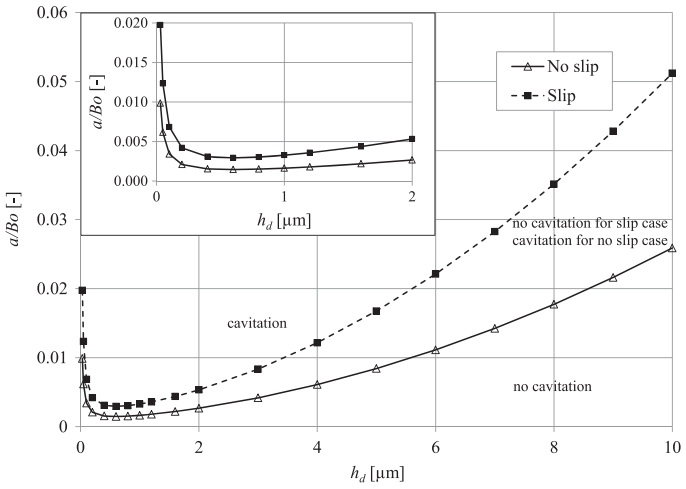

Figure 9. Cavitation as a function of inlet land width *a*/*Bo* and pocket depth *hd*. The profiles are calculated for $h_o = 1.0 \times 10^{-6}$ m, $a = 0.004$ m, $b = 0.006$ m, $B_o = 0.02$ m, $\alpha = 0.02$ m^{2}s/kg, and $P_{cav} = 0$ kPa. The insert shows the predicted *a*/*Bo* for low values of h_d (i.e. up to 2.0×10^{-6} m).

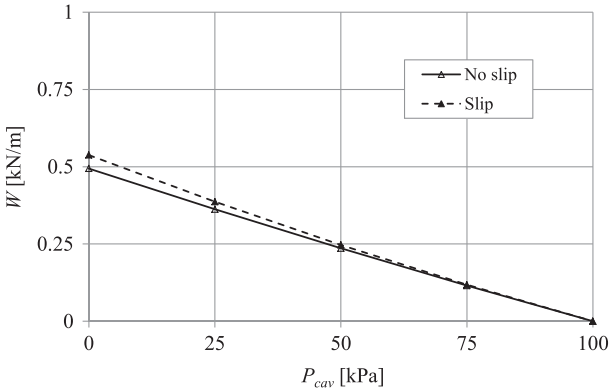

Figure 10. Effect of cavitation pressure on the load support. The profiles are calculated for $h_o = 1.0 \times 10^{-6}$ m, $h_d = 5.0 \times 10^{-6}$ m, $a = 0.004$ m, $b = 0.006$ m, $B_o = 0.02$ m, $\alpha = 0.02$ m^{2}s/kg.

in load support is linearly with cavitation pressure. When the cavitation pressure equals atmospheric pressure, the predicted load support falls to zero. It indicates that the slip has just an effect when the cavitation pressure is quite low as well as in the no-slip case to make inlet suction to occur.

From Figure 11, it can be seen that for all values of pocket depth h_d, increasing the slip coefficient shows a reduction in friction, while increasing the α more than a specified number hardly changes that performance, there is a decrease in friction in the range for the slip coefficient α from 0.02 to 0.10 m^{2}s/kg.

DOI: 10.1002/ls

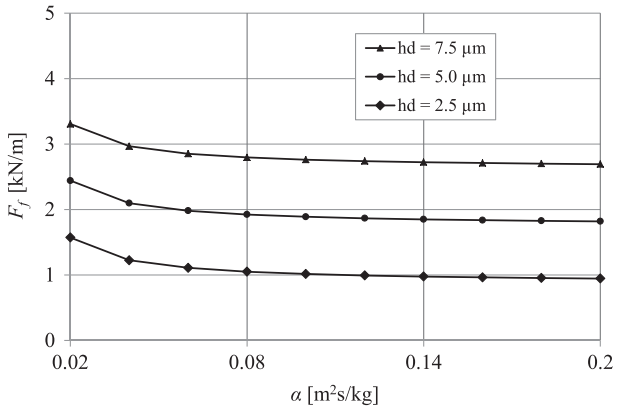

Figure 11. Effect of slip coefficient on friction force. The profiles are calculated for $h_o = 1.0 \times 10^{-6}$ m, $a = 0.004$ m, $b = 0.006$ m, $B_o = 0.02$ m.

Figure 12 shows the influence of the cavitation pressure on friction. For a no-slip bearing, it can be observed that the cavitation pressure does not have an effect on the friction and hardly for the slip bearing. It can be noted from this figure, the friction predicted for a bearing with slip is 50 to 200 times lower that the no-slip bearing depending on the cavitation pressure. In relation to the friction reduction by full slip, some of the earliest works[26–28,31] revealed the same result.

Figure 13 plots friction F_f versus the minimum film thickness h_o. It can be seen that the introduction of slip to the textured bearing results in low friction both for low h_o and high h_o. Increasing the h_o to the value of 1.0×10^{-6} m does not affect the friction very much. However, after h_o of 1.0×10^{-6} m, the friction decreases significantly. This phenomena is opposite with the no-slip textured bearing. For low h_o, the friction is very large. Only for high h_o (i.e. 1.0×10^{-4} m and above), the prediction of such

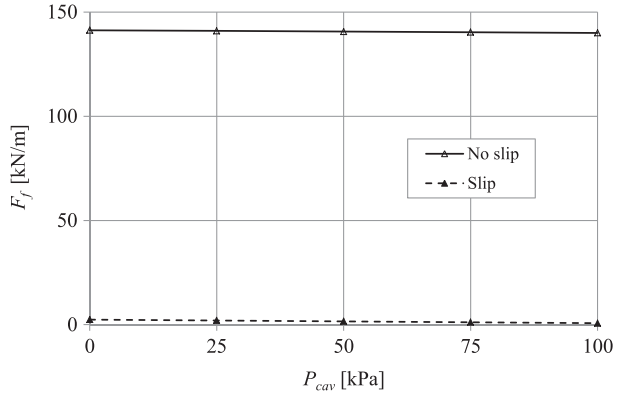

Figure 12. Effect of cavitation pressure on friction for a bearing with $h_o = 1.0 \times 10^{-6}$ m, $h_d = 5.0 \times 10^{-6}$ m, $a = 0.004$ m, $b = 0.006$ m, $B_o = 0.02$ m, $\alpha = 0.02$ m²s/kg.

DOI: 10.1002/ls

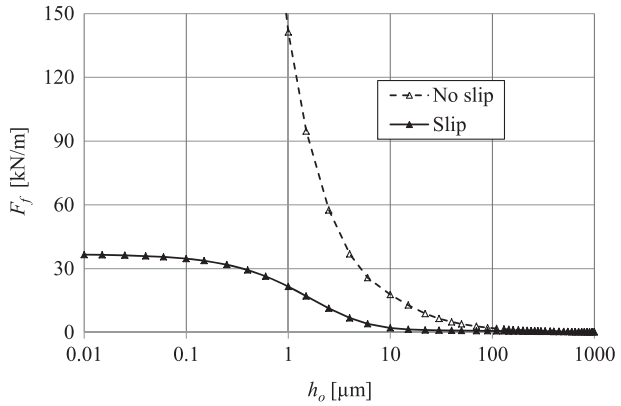

Figure 13. Influence of the minimal film thickness h_o on friction F_f for bearing with $h_d = 5.0 \times 10^{-6}$ m, $a = 0.004$ m, $b = 0.006$ m, $B_o = 0.02$ m, $\alpha = 0.02$ m^{2}s/kg.

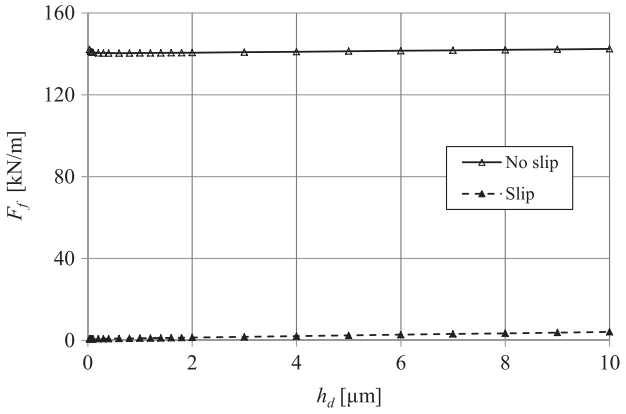

Figure 14. Influence of the pocket depth h_d on friction F_f for bearing with $h_o = 1.0 \times 10^{-6}$ m, $a = 0.004$ m, $b = 0.006$ m, $B_o = 0.02$ m, $\alpha = 0.02$ m^{2}s/kg.

bearing achieves similar values with that of a textured bearing with slip. It also indicates that adding slip to a textured bearing with high h_o does not have a significant effect in reducing friction.

Figure 14 presents the influence of h_d on the friction F_f. It can be observed that friction is not affected by the pocket depth significantly both for the case of a slip and no-slip textured bearing. However, as shown in previous results, slip generates very low friction.

Figure 15 shows friction force F_f versus b/B_o. It can be seen that slip leads to the reduction in friction for two values of h_d and b/B_o considered here. The predicted reduction in friction is spectacular, both for high b ($b = 0.35\ B_o$ in this case) and low b ($b = 0.01\ B_o$). For example, for high b, the friction reduction resulted by applying the slip is up to 8856% and 4190%, respectively, for $h_d = 2.5 \times 10^{-6}$ m and 7.5×10^{-6} m compared with bearing without slip. The same order of the friction reduction is also found for low b. It indicates that introducing slip in sliding bearing is advisable with respect to the friction force reduction.

DOI: 10.1002/ls

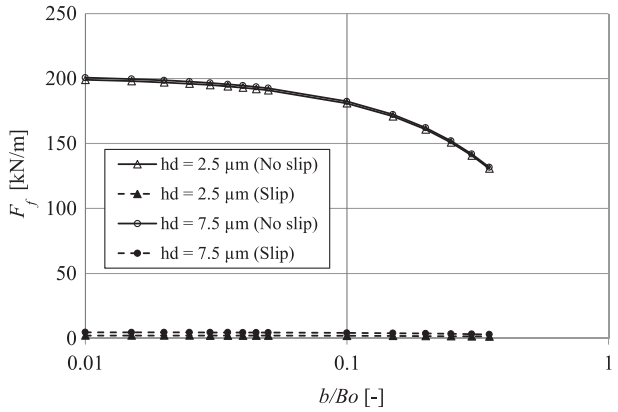

Figure 15. Plot of friction force F_f versus b/B_o for a bearing with $h_o = 1.0 \times 10^{-6}$ m, $a = 0.004$ m, $B_o = 0.02$ m, $\alpha = 0.02$ m^{2}s/kg.

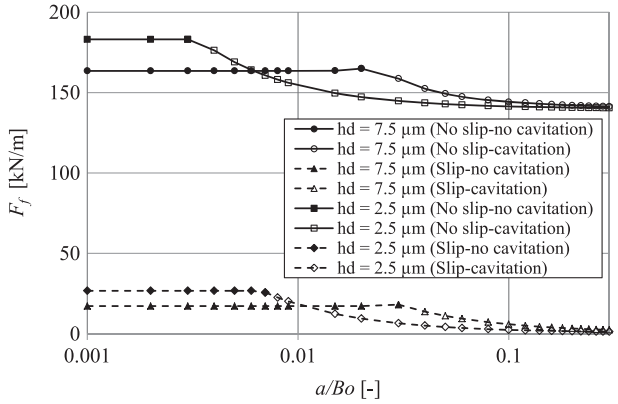

Figure 16. Plot of F_f versus inlet land width a/B_o for bearing with $h_o = 1.0 \times 10^{-6}$ m, $b = 0.006$ m, $B_o = 0.02$ m, $\alpha = 0.02$ m^{2}s/kg.

Figure 16 depicts how friction varies with inlet length a/B_o for a pocketed bearing of interest with $h_o = 1.0 \times 10^{-6}$ m, $b = 0.006$ m and $B_o = 0.02$ m. For the slip bearing, α is set to 0.02 m^{2}s/kg. It can be observed that increasing the inlet length a/B_o to the certain value leads to the presence of cavitation, both for the no-slip and slip cases for two values of h_d considered. For the slip bearing, the value of 'transition' from no-cavitation to cavitation is higher than that for the no-slip bearing for the two h_d values, extending the inlet length combined with slip is still able to prevent cavitation.

CONCLUSIONS

This paper focused on the possibility of inlet suction by the use of pockets in a bearing with and without boundary slip. A 1-D analytical model for a pocketed bearing with boundary slip has been

DOI: 10.1002/ls

developed, and the effect of the boundary slip on the hydrodynamic performance (load support and friction) has been analysed. The following conclusions summarise the results of the present study:

1. The cavitation pressure has a huge impact on performance characteristics both for the slip pocketed bearing and no-slip pocketed one. Setting the cavitation pressure to be very low does help in improving the load support and reducing friction.
2. The best performance can be achieved when the configuration of a pocket bearing with slip has a small ratio of inlet to outlet pad length.
3. The most significant finding is that introducing slip in pocketed bearings enhances the effect of 'suction' lubricant into the bearing, and therefore increases the lubricant flow. Consequently, this improves the pressure generation within the bearing compared to the no-slip pocketed bearing.

REFERENCES

1. Etsion I, Halperin G, Brizmer V, Kligerman Y. Experimental investigation of laser surface textured parallel thrust bearing. *Tribology Letters* 2004; **17**:295–300.
2. Kovalchenko A, Ajayi O, Erdemir A, Fenske G, Etsion I. The effect of laser surface texturing on transitions in lubrication regimes during unidirectional sliding contact. *Tribology International* 2005; **38**:219–225.
3. Etsion I, Halperin G. A laser surface textured hydrostatic mechanical seal. *STLE Tribology Transactions* 2002; **45**:430–434.
4. Ryk G, Kligerman Y, Etsion I. Experimental investigation of laser surface texturing for reciprocating automotive components. *STLE Tribology Transactions* 2002; **45**:444–449.
5. Arghir M, Roucou N, Helene M, Frene J. Theoretical analysis of the incompressible laminar flow in a macro-roughness cell. *ASME Journal of Tribology* 2003; **125**:309–318.
6. Sahlin F, Glavatskih SB, Almqvist T, Larsson R. Two-dimensional CFD-analysis of micro-patterned surfaces in hydrodynamic lubrication. *ASME Journal of Tribology* 2005; **127**:96–102.
7. Brajdic-Mitidieri P, Gosman AD, Loannides E, Spikes HA. CFD analysis of a low friction pocketed pad bearing. *ASME Journal of Tribology* 2005; **127**:803–812.
8. Kligerman Y, Etsion I, Shinkarenko A. Improving tribological performance of piston rings by partial surface texturing. *ASME Journal of Tribology* 2005; **127**:632–638.
9. Fowell M, Olver AV, Gosman AD, Spikes HA, Pegg I. Entrainment and Inlet Suction: two mechanisms of hydrodynamic lubrication in textured bearings. *ASME Journal of Tribology* 2007; **129**:337–347.
10. Dobrica MB, Fillon M. About the validity of Reynolds equation and inertia effects in textured sliders of infinite width. *Proceedings of the imeche part j journal of engineering tribology* 2009; **223**:69–78.
11. Han J, Fang L, Sun J, Ge S. Hydrodynamic lubrication of microdimple textured surface using three-dimensional CFD. *Tribology Transactions* 2010; **53**(6):860–870.
12. Zhu Y, Granick S. Limits of the hydrodynamic of no-slip boundary condition. *Physical Review Letters* 2002; **88**(10):106102.
13. Zhu Y, Granick S. No-slip boundary condition switches to partial slip when fluid contacts surfactant. *Langmuir* 2002; **18**:10058–10063.
14. Bonaccurso E, Kappl M, Butt HJ. Hydrodynamic force measurement: boundary slip of water on hydrophilic surfaces and electrokinetic effects. *Physical Review Letters* 2002; **88**:076103.
15. Kalin M, Polajnar M. The effect of wetting and surface energy on the friction and slip in oil-lubricated contacts. *Tribology Letters* 2013; **52**:185–194.
16. Jin J, Zhang G, Wang X. Experiment and simulation on lubrication performance of EMP journal bearing. *Journal of Shanghai University* 2004; **8**:85–89.
17. Choo JH, Glovnea R, Forrest A, Spikes HA. A low friction bearing based on liquid slip at the wall. *Journal of Tribology* 2007; **129**:611–620.
18. Choo JH, Spikes HA, Ratoi M, Glovnea R, Forrest A. Friction reduction in low-load hydrodynamic lubrication with a hydrophobic surface. *Tribology International* 2007; **40**:154–159.
19. Reyes JS, Archer LA. Interficial slip violations in polymer solution: role of microscale surface roughness. *Langmuir* 2003; **19**:3304–3312.

DOI: 10.1002/ls

20. Leong JY, Reddyhoff T, Sinha SK, Holmes AS, Spikes HA. Hydrodynamic friction reduction in a MAC–hexadecane lubricated MEMS contact. *Tribology Letters* 2013; **49**:217–225.
21. Ku ISY, Reddyhoff T, Wayte R, Holmes AS, Choo JH, Spikes HA. Lubrication of microelectromechanical devices using liquids of different viscosities. *Journal of Tribology* 2012; **134**:1–7.
22. Delgado MA, Franco JM, Partal P, Gallegos C. Experimental study of grease flow in pipelines: wall slip and air entrainment effect. *Chemical Engineering and Processing* 2005; **44**:805–817.
23. Ruiz-viera MJ, Delgado MA, Franco JM, Gallegos C. Evaluation of wall slip effect in the lubricating grease/ air two-phase flow along pipeline. *Journal Non-Newtonian Fluid Mechanics* 2006; **39**:190–196.
24. Salant RF, Fortier AE. Numerical analysis of a slider bearing with a heterogeneous slip/no-slip surface. *Tribology Transactions* 2004; **47**:328–334.
25. Wu CW, Ma GJ, Zhou P. Low friction and high load support capacity of slider bearing with a mixed slip surface. *ASME Journal of Tribology* 2006; **128**:904–907.
26. Ma GJ, Wu CW, Zhou P. Hydrodynamic of slip wedge and optimization of surface slip property. *Science China Physics, Mechanics &Astronomy* 2007; **50**:321–330.
27. Ma GJ, Wu CW, Zhou P. Influence of wall slip on the hydrodynamic behavior of a two-dimensional slider bearing. *Acta Mechanica Sinica* 2007; **23**:655–66.
28. Bayada G, Meurisse MH. Impact of the cavitation model on the theoretical performance of heterogeneous slip/no-slip engineered contacts in hydrodynamic conditions. *Proceedings of the imeche part j journal of engineering tribology* 2009; **223**:371–381.
29. Rao TVVLN. Analysis of single-grooved slider and journal bearing with partial slip surface. *ASME Journal of Tribology* 2010; **132**:014501-1–014501-7.
30. Aurelian F, Patrick M, Mohamed H. Wall slip effects in (elasto) hydrodynamic journal bearing. *Tribology International* 2011; **44**:868–877.
31. Tauviqirrahman M, Ismail R, Jamari J, Schipper DJ. Combined effect of texturing and boundary slippage in lubricated sliding contacts. *Tribology International* 2013; **66**:274–281.
32. Tauviqirrahman M, Ismail R, Jamari J, Schipper DJ. A study of surface texturing and boundary slip on improving the load support of lubricated parallel sliding contacts. *Acta Mechanica* 2013; **224**:365–381.
33. Tauviqirrahman M, Muchammad JJ, Schipper DJ. Numerical study of the load carrying capacity of lubricated parallel sliding textured surfaces including wall slip. *Tribology Transactions* 2013; **57**(1):134–145.
34. Tauviqirrahman M, Muchammad IR, Jamari J, Schipper DJ. Friction characteristics of liquid lubricated MEMS with deterministic boundary slippage. *Jurnal Teknologi* 2014; **66**(3):75–80.
35. Wang L-l, Lu C-h. Numerical analysis of spiral oil wedge sleeve bearing including cavitation and wall slip effect. *Lubrication science* 2015; **27**(3):193–207.

APPENDIX

The analysis below is based on continuity of flow through the bearing and uses the terminology shown in Figure 1. For the condition in which the slip velocity both at the moving and stationary solid–liquid interface, respectively, follows the Navier slip model, the corresponding flow rate equation can be expressed as:[31]

$$q_x = -\frac{\partial}{\partial x}\left(\frac{h^3}{12\mu}\frac{h^2+4\mu h(\alpha_h+\alpha_s)+12\mu^2\alpha_h\alpha_s}{h(h+\mu(\alpha_h+\alpha_s))}\frac{\partial p}{\partial x}\right)+\frac{U}{2}\frac{\partial}{\partial x}\left(\frac{h^2+2\mu h\alpha_h}{h+\mu(\alpha_h+\alpha_s)}\right) + \frac{h}{2\mu}\frac{\partial p}{\partial x}\frac{\partial h}{\partial x}\frac{\mu h\alpha_h+2\mu^2\alpha_h\alpha_s}{h+\mu(\alpha_h+\alpha_s)}-U\frac{\partial h}{\partial x}\frac{\mu\alpha_h}{h+\mu(\alpha_h+\alpha_s)}. \tag{A.1}$$

If slip is only present on the stationary surface ($\alpha_s = 0$ but $\alpha_h \neq 0$), equation A.1 will reduce to:

DOI: 10.1002/ls

$$q_x = -\frac{\partial}{\partial x}\left(\frac{h^3}{12\mu}\frac{\partial p}{\partial x}\frac{h^2+4\mu h\alpha_h}{h(h+\mu\alpha_h)}\right)+\frac{U}{2}\frac{\partial}{\partial x}\left(\frac{h^2+2\mu h\alpha_h}{2(h+\mu\alpha_h)}\right). \tag{A.2}$$

For the first order Reynolds equation, the flow rate is given:

$$q_x = \frac{U}{2}\frac{h^2+2\mu h\alpha_h}{h+\mu\alpha_h}-\frac{h^3}{12\mu}\frac{h+4\mu\alpha_h}{h+\mu\alpha_h}\frac{dP}{dx}. \tag{A.3}$$

A.1 No cavitation in recess

A.1.1 Load support

For the areas of the bearing containing parallel surfaces the film thickness h is constant, the pressure gradient must be linear (see equation A.3). Equation A.3 can be modified for each region of the bearing to

$$q_{AB} = \frac{U}{2}\frac{h_o^2+2\mu h_o\alpha_h}{h_o+\mu\alpha_h}-\frac{h_o^3}{12\mu}\frac{h_o+4\mu\alpha_h}{h_o+\mu\alpha_h}\left(\frac{P_2-P_{atm}}{a}\right) \tag{A.4}$$

$$q_{BC} = \frac{U}{2}\frac{h_p^2+2\mu h_p\alpha_h}{h_p+\mu\alpha_h}-\frac{h_p^3}{12\mu}\frac{h_p+4\mu\alpha_h}{h_p+\mu\alpha_h}\left(\frac{P_3-P_2}{b}\right) \tag{A.5}$$

$$q_{CD} = \frac{U}{2}\frac{h_o^2+2\mu h_o\alpha_h}{h_o+\mu\alpha_h}-\frac{h_o^3}{12\mu}\frac{h_o+4\mu\alpha_h}{h_o+\mu\alpha_h}\left(\frac{P_{atm}-P_3}{c}\right) \tag{A.6}$$

with one condition $q_{AB}=q_{BC}=q_{CD}$ based on volume conservation.

When q_{AB} is set to be equal to q_{CD}

$$\begin{aligned}&\frac{U}{2}\frac{h_o^2+2\mu h_o\alpha_h}{h_o+\mu\alpha_h}-\frac{h_o^3}{12\mu}\frac{h_o+4\mu\alpha_h}{h_o+\mu\alpha_h}\left(\frac{P_2-P_{atm}}{a}\right)=\\&\frac{U}{2}\frac{h_o^2+2\mu h_o\alpha_h}{h_o+\mu\alpha_h}-\frac{h_o^3}{12\mu}\frac{h_o+4\mu\alpha_h}{h_o+\mu\alpha_h}\left(\frac{P_{atm}-P_3}{c}\right)\end{aligned} \tag{A.7}$$

$$\left(\frac{P_2-P_{atm}}{a}\right)=\left(\frac{P_{atm}-P_3}{c}\right) \tag{A.8}$$

For the non cavitating case, P_2 is unknown. Equating flow rate in inlet land and recess, $q_{AB}=q_{BC}$

DOI: 10.1002/ls

$$\begin{aligned}&\frac{U}{2}\frac{h_o^2+2\mu h_o\alpha_h}{h_o+\mu\alpha_h}-\frac{h_o^3}{12\mu}\frac{h_o+4\mu\alpha_h}{h_o+\mu\alpha_h}\left(\frac{P_2-P_{atm}}{a}\right)=\\&\frac{U}{2}\frac{h_p^2+2\mu h_p\alpha_h}{h_p+\mu\alpha_h}-\frac{h_p^3}{12\mu}\frac{h_p+4\mu\alpha_h}{h_p+\mu\alpha_h}\left(\frac{P_3-P_2}{b}\right)\end{aligned}\tag{A.9}$$

If, $K_o=\frac{\mu\alpha_h}{h_o+\mu\alpha_h}$ and, $K_p=\frac{\mu\alpha_h}{h_p+\mu\alpha_h}$ then

$$\begin{aligned}&\frac{Uh_o}{2}(1+K_o)-\frac{h_o^3}{12\mu}(1+3K_o)\left(\frac{P_2-P_{atm}}{a}\right)=\\&\frac{Uh_p}{2}(1+K_p)-\frac{h_p^3}{12\mu}(1+3K_p)\left(\frac{P_3-P_2}{b}\right)\end{aligned}\tag{A.10}$$

From equation A.8, it is known that $P_3=P_{atm}-\frac{c}{a}(P_2-P_{atm})$; therefore,

$$\left(\frac{P_3-P_2}{b}\right)=\frac{ab+bc}{ab^2}(P_{atm}-P_2).\tag{A.11}$$

Substitution of equation A.8 in equation A.9 gives

$$\begin{aligned}&P_2\left[\left(h_p^3+3h_p^3K_p\right)\frac{ab+bc}{ab^2}+\left(\frac{h_o^3+3h_o^3K_o}{a}\right)\right]=\\&P_{atm}\left[\left(h_p^3+3h_p^3K_p\right)\frac{ab+bc}{ab^2}+\left(\frac{h_o^3+3h_o^3K_o}{a}\right)\right]\\&-6\mu U\left[\left(h_p+h_pK_p\right)-\left(h_o+K_o\right)\right]\end{aligned}\tag{A.12}$$

where

$$\begin{aligned}C_p^*&=h_p^3+3h_p^3K_p\\C_o^*&=h_o^3+3h_o^3K_o\\C_p&=h_p+h_pK_p\\C_o&=h_o+h_oK_o.\end{aligned}$$

Combining equations A.11 and A.12 to eliminate *P3* gives

$$P_2\left(\frac{ab+bc}{ab^2}C_p^*+\frac{C_o^*}{a}\right)=P_{atm}\left(\frac{ab+bc}{ab^2}C_p^*+\frac{C_o^*}{a}\right)-6\mu U\left(C_p-C_o\right)\tag{A.13}$$

and thus,

DOI: 10.1002/ls

$$P_3 = P_{atm} + \frac{6\mu U\left(C_p - C_o\right)bc}{aC_p^* + cC_p^* + bC_o^*} \tag{A.14}$$

Due to linearity between the pressure gradient in the inlet and outlet lands and in the recess, each of three areas of the bearing has a triangular pressure distribution that can be simply integrated to determine the load support. Therefore, the total normal force reads:

$$W = W_{AB} + W_{BC} + W_{CD} - P_{atm}(a + b + c) \tag{A.15}$$

$$W = -\frac{6\mu U\left(C_p - C_o\right)ab}{aC_p^* + cC_p^* + bC_o^*}\left(\frac{a+b}{2}\right) + \frac{6\mu U\left(C_p - C_o\right)bc}{aC_p^* + cC_p^* + bC_o^*}\left(\frac{b+c}{2}\right). \tag{A.16}$$

Finally, the load support reads

$$W = \frac{6\mu U\left(C_p - C_o\right)}{C_p^*}\frac{b}{2}\left(\frac{c^2 - ab - a^2 + bc}{a + c + b\frac{C_o^*}{C_p^*}}\right). \tag{A.17}$$

A.1.2 Shear stress

The shear stress at the lower surface can be derived as follows:

$$\tau = -\frac{\mu U}{h + \mu\alpha_h} - \frac{h}{2}\frac{\partial P}{\partial x}\frac{h + 2\mu\alpha_h}{h + \mu\alpha_h}. \tag{A.18}$$

For the case of no cavitation, the friction force reads:

$$F_f = F_{fAB} + F_{fBC} + F_{fCD} \tag{A.19}$$

$$F_f = -\mu U\left[\frac{a}{h_o + \mu\alpha_h} + \frac{c}{h_o + \mu\alpha_h} + \frac{b}{h_p + \mu\alpha_h} + \left(\frac{3\left(C_p - C_o\right)^2 b(a+c)}{aC_p^* + cC_p^* + bC_o^*}\right)\right]. \tag{A.20}$$

A.2 Cavitation in recess

A.2.1 Load support

For the case of cavitation in recess, P_2 is assumed to be equal to P_{cav}, so $q_{AB} = q_{B'C}$ gives

$$\begin{aligned}&\frac{Uh_o}{2}(1 + K_o) - \frac{h_o^3}{12\mu}(1 + 3K_o)\left(\frac{P_{cav} - P_{atm}}{a}\right) = \\ &\frac{Uh_p}{2}\left(1 + K_p\right) - \frac{h_p^3}{12\mu}\left(1 + 3K_p\right)\left(\frac{P_3 - P_{cav}}{X_b}\right)\end{aligned} \tag{A.21}$$

where

DOI: 10.1002/ls

$$X_b = \frac{C_p^*(P_3 - P_{cav})}{6\mu U\left(C_p - C_o\right) - C_o^*\left(\frac{P_{atm}-P_{cav}}{a}\right)}. \tag{A.22}$$

It should be noted that for the cavitation zone, the pressure must be integrated separately, i.e. the non cavitated area and cavitated area of the recess, so the total load support reads

$$W = W_{AB} + W_{BB'} + W_{B'C} + W_{CD} - P_{atm}(a + b + c) \tag{A.23}$$

$$W = \left[P_{atm}a + \frac{a^2}{2a}(P_{cav} - P_{atm})\right] + [P_{cav}b(1 - X_b)]$$

$$+\left[P_{cav}X_b + \frac{6\mu U(X_b)^2}{2C_p^*}\left(C_p - C_o\right) + \frac{C_o^*(X_b)^2}{2aC_p^*}(P_{cav} - P_{atm})\right] \tag{A.24}$$

$$+\left[P_{atm}c - \frac{c^2}{2a}(P_{cav} - P_{atm})\right] - P_{atm}(a + b + c).$$

A.2.2 Friction force

$$F_f = F_{fAB} + F_{fBB'+}F_{fB'C} + F_{fCD} \tag{A.25}$$

$$F_f = -\left\{\mu U\left[\frac{a}{h_o + \mu\alpha_h} + \frac{c}{h_o + \mu\alpha_h} + \frac{X_b}{h_p + \mu\alpha_h}\right] + \left[\left(\frac{C_p}{2} - \frac{C_o}{2}\right)\left(1 + \frac{c}{a}\right)(P_{atm} - P_{cav})\right]\right\}. \tag{A.26}$$

DOI: 10.1002/ls